Nonequilibrium Fluctuations of Global Warming

Nonequilibrium Fluctuations of Global Warming

JUN YIN,[a,b] AMILCARE PORPORATO,[c,d] AND LAMBERTO RONDONI[e,f]

[a] *Department of Hydrometeorology, Nanjing University of Information Science and Technology, Nanjing, China*
[b] *Key Laboratory of Hydrometeorological Disaster Mechanism and Warning of Ministry of Water Resources, Institute of Soil Health and Climate-Smart Agriculture, Nanjing University of Information Science and Technology, Nanjing, China*
[c] *Department of Civil and Environmental Engineering, Princeton University, Princeton, New Jersey*
[d] *High Meadows Environmental Institute, Princeton University, Princeton, New Jersey*
[e] *Dipartimento di Scienze Matematiche, Politecnico di Torino, Turin, Italy*
[f] *INFN, Sezione di Torino, Torino, Italy*

(Manuscript received 8 May 2023, in final form 4 January 2024, accepted 12 February 2024)

ABSTRACT: While the warming trends of Earth's mean temperature are evident at climatological scales, the local temperature at shorter time scales are highly fluctuating. Here we show that the probabilities of such fluctuations are characterized by a special symmetry typical of small systems out of equilibrium. Their nearly universal properties are linked to the fluctuation theorem and reveal that the progressive warming is accompanied by growing asymmetry of temperature distributions. These statistics allow us to project the global temperature variability in the near future, in line with predictions from climate models, providing original insight about future extremes.

KEYWORDS: Surface temperature; Thermodynamics; Statistics; Anomalies; Climate variability

1. Introduction

Climate change tends to be more evident in processes that integrate temperature variability at long time scales, such as glacial melting and sea level rise (Tebaldi et al. 2021), while it may be somewhat masked by fluctuations when focusing on quantities, such as temperature and precipitation extremes, which vary more erratically (Hansen et al. 2012; Trenberth et al. 2015). Even the mean annual temperature, which is typically used as a measure of climate change progression, may be deceiving due to its strong space–time variability: for example, in 2020—one of the hottest years on record—nearly half (49.1%) of Earth was actually colder than the previous year (see Fig. 1a). However, when such fluctuations are looked at more carefully, they become an asset for robust projections. Besides changes in the central tendency statistics, climate change is also altering the frequency and intensity of extreme events of several quantities, including temperature and other thermodynamic, dynamic and hydrological variables (e.g., Seager et al. 2010; Donat and Alexander 2012; Ruff and Neelin 2012). Understanding the interaction between shifts in the mean and changes in the distributions of hydroclimatic variables is imperative to reliable prediction of future climates.

The fact that the climate system is a nonlinear open system, inherently chaotic in both space and time (Bohr and van de Water 1994; Cross and Hohenberg 1994) makes the understanding of the multiscale nature of Earth's climatic fluctuations particularly challenging. The scale dependence of rising temperature has long been recognized (Marotzke and Forster 2015). The overall warming trends, driven by the growing concentration of greenhouse gases in the atmosphere, are embedded within the warming and cooling patterns controlled by the large-scale circulation (e.g., at synoptic and interannual scales) (Lu et al. 2007; Seager et al. 2010). Thus, it is not surprising that the warmer-than-usual temperature in the central and eastern tropical Pacific, identified as El Niño, is typically accompanied by cooler temperatures in the nearby North and South Pacific as well as in the remote regions of northern Europe (Diaz et al. 2001; Brönnimann et al. 2007).

While early contributions focused on trends and shifts in mean and variance, recently more attention has been devoted to higher-order moments and distributional tails and how these are modulated by advection and large-scale modes of climate variability (Stefanova et al. 2013). The structure of the fluctuations plays a leading role in indicating how locations will be affected by a warming climate. Huybers et al. (2014) suggested that warming is unlikely to result in a simple distribution shift due to nonlinear interactions between the mean and tails, resulting in departures from normality and the degree to which extreme changes are amplified relative to the mean. Temperature distributions were reported to become skewed toward the hotter part of the distribution, leading to the conclusion that the distribution of global daily temperatures has become more extreme (Donat and Alexander 2012), while Lewis and King (2017) found a consistent skew in daily temperatures toward hot extremes. The relation between temperature skewness shifts and changes in atmospheric dynamics (e.g., meridional advection) is crucial for deciphering future climate change (Tamarin-Brodsky et al. 2019).

Denotes content that is immediately available upon publication as open access.

Supplemental information related to this paper is available at the Journals Online website: https://doi.org/10.1175/JCLI-D-23-0273.s1.

Corresponding author: Amilcare Porporato, aporpora@princeton.edu

DOI: 10.1175/JCLI-D-23-0273.1

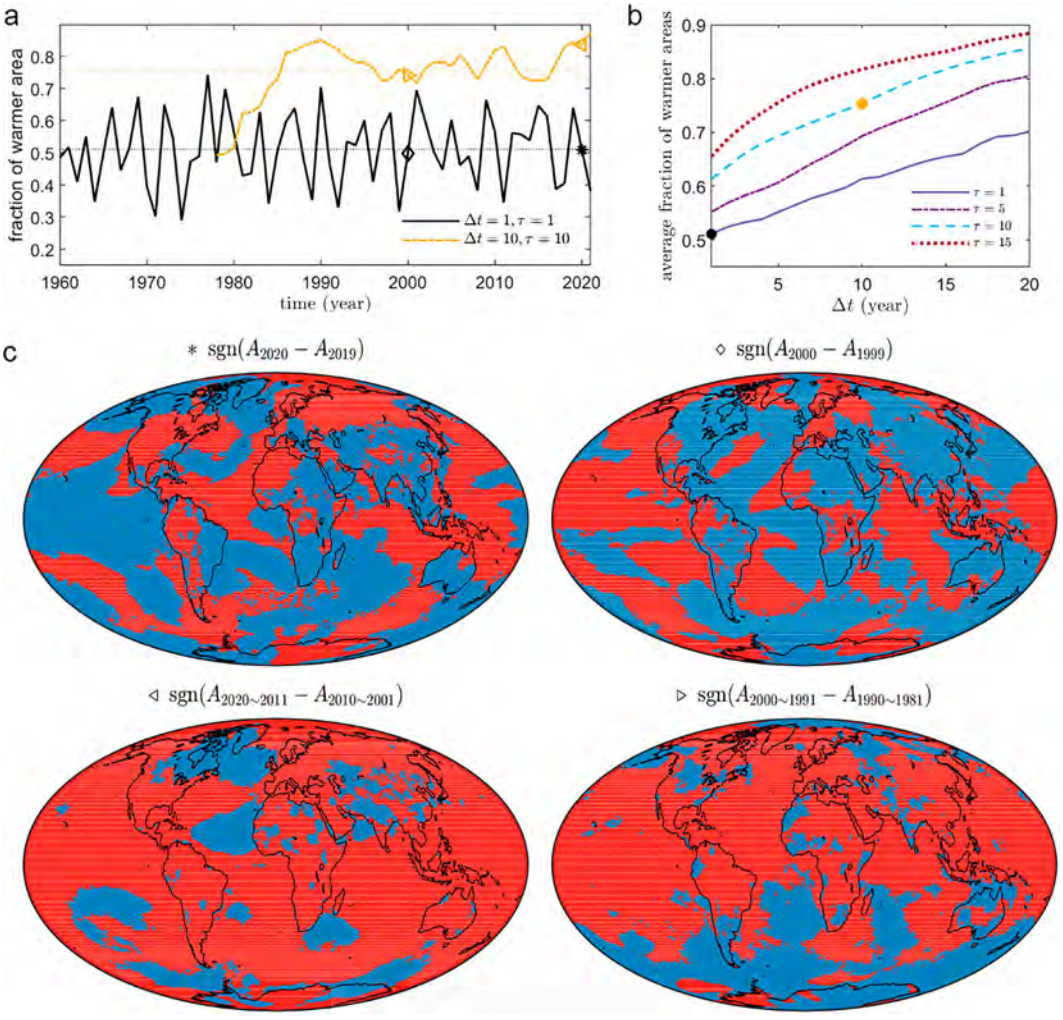

FIG. 1. Multiscale analysis of global warming fluctuations. (a) Fraction of Earth's surface having annual temperatures higher than the previous year (black solid lines) or decade-average temperatures higher than the previous decade (yellow dash–dotted lines). (b) Average fraction of warmer areas with the varying time difference (Δt) and averaging windows (τ). The black and yellow dots in (b) correspond to the black and yellow horizontal dashed lines in (a), respectively. (c) Geographical distributions of warmer (red) and colder (blue) regions with different averaging windows and time differences. The areal fraction of the total warmer regions in (c) are marked in (a) with the same star, diamond, and left and right triangles. Results are based on ERA5; see similar patterns for other data sources in Fig. S2.

To better understand the structure of Earth's global warming fluctuations, here we draw from recent advances in statistical mechanics on the structure of fluctuations of nonequilibrium phenomena (Evans et al. 1993; Gallavotti and Cohen 1995; Crooks 1999; Evans and Searles 2002; Jarzynski 2004; Marconi et al. 2008; Evans and Morriss 2008; Seifert 2012; Gallavotti 2014). Initially concerning the entropy production of chaotic many particle systems, such theories have derived novel symmetries that point to a certain degree of universality in the nonequilibrium fluctuations of observables and in the response to perturbations of large as well as "small" systems. In particular, small systems are characterized by fluctuations of size comparable to the observed average signals, hence they cannot be neglected. A deeper understanding of the macroscopic properties of such systems has emerged from leveraging the statistics of instantaneous microscopic events, which often look totally random and per se do not appear to have a direction of time but, when averaged in time, they reveal a preferred direction for the overall evolution. This can be used to quantify the degree of asymmetry and irreversibility of the system, and to identify an asymptotic universal behavior verifying scaling relationships that help extrapolate it to long times.

2. A "microscopic" view of global warming

A distinctive feature of Earth's hydroclimatic fluctuations is that the largest ones are comparable with Earth's size (Klein 2010), effectively rendering its behavior like the one of "small

systems" from the point of view of statistical mechanics. Earth is driven out of equilibrium by input of low-entropy radiation and an outgoing high-entropy longwave radiation (Kleidon 2016). Its dynamics fluctuate in space and time displaying complex behavior (Alexandrov et al. 2021). According to the small system point of view, the observed statistics of entropy production should reveal special symmetries linking warming (which correspond to increased entropy production) and cooling events around their positive average values. Normally, fluctuation relations can be verified when a macroscopic object is observed on a microscopic scale (e.g., Bonaldi et al. 2009); however, the theory of nonequilibrium fluctuations is of particular interest in the case of systems with constituting elements interacting on scales comparable with those of the overall system, because fluctuations are then *observable* on the same scale of the global phenomenon. Dissipative complex phenomena such as turbulence (Ciliberto and Laroche 1998; Gallavotti et al. 2004; Porporato et al. 2020) and the behavior of bacteria (Bechinger et al. 2016) have been shown to follow similar rules. This is consistent with the small system picture, because the relevant elementary constituents (eddies or single bacteria) are moderately numerous and interact on the scale of the whole system. The ensuing response theory of both near- and far-from-equilibrium fluctuations (Ghil and Lucarini 2020) is a promising framework to analyze the macroscopic patterns of global warming and shed light into Earth's climate dynamics.

To analyze Earth's fluctuating response to climate change, here we first consider an illustrative example of global temperature anomalies at different temporal scales. As shown in the global maps of Fig. 1, when focusing on short time scales, nearly half of Earth has positive anomaly differences (black solid lines in Fig. 1a) and the spatial distribution of warmer or cooler regions changes almost randomly (e.g., Fig. 1c). Even for the North Pole, one of the fastest-warming regions (Bekryaev et al. 2010; Stuecker et al. 2018), still only half the region is getting warmer each year (see Fig. S1 in the online supplemental material). However, as the averaging window and time difference are increased, a significant portion of Earth appears to be getting warmer (yellow dash–dotted lines in Fig. 1a and spatial patterns in Fig. 1c). Similar results are obtained from other climate data (combined sea surface temperature over the ocean and near-surface air temperature over the land; see Fig. S2). The warming signal becomes stronger with longer time scales (see Fig. 1b) as the fluctuations get averaged out.

While this scale-dependent global warming pattern has been intensely investigated in climate science (e.g., Klein 2010; Franzke et al. 2020), less effort has been focused on coherently quantifying such cross-scale fluctuations and its similarity with a small system out of equilibrium. Toward this goal, we consider the temperature anomalies a, defined as the deviation from the average temperature over 1959–2014, covering a period with available data from both reanalysis and climate model outputs. The choice of base period does not change the asymmetric patterns discovered in this study (see Fig. S3 for results based on different base periods). The local anomaly is averaged over a time window τ:

$$A(t;\tau)=\frac{1}{\tau}\int_{t-\tau}^{t}a(t)dt, \tag{1}$$

and also compared between two periods separated by a time difference Δt:

$$\Delta A(t;\tau,\Delta t)=A(t;\tau)-A(t-\Delta t;\tau). \tag{2}$$

The results show that the global distributions of both A and ΔA exhibit clear structures, which are robust when changing averaging and differencing time windows, consistently with the theory of nonequilibrium fluctuations. The obtained probability density functions (PDF) consistently presents double exponential tails (straight lines in the logarithmic plots, see Figs. 2a,c), which become more evident for longer averaging windows. The shape of the distributions is well captured by asymmetric double exponential distributions (Kozubowski and Podgórski 2000; Yu and Zhang 2005), with PDF:

$$f(x;m,\beta_1,\beta_2)=\begin{cases}\beta_0\exp[-(x-m)/\beta_1], & x>m\\ \beta_0\exp[(x-m)/\beta_2], & x\le m\end{cases}, \tag{3}$$

where the random variable x may refer to either A or ΔA, m is the mode, β_1 and β_2 are the exponents for the right and left tails, and $\beta_0=1/(\beta_1+\beta_2)$. The differences between these double exponential distributions and the Gaussian distributions conventionally used in climatology can be visualized by quantile–quantile plots. As shown in Fig. 3, deviations from normality for extreme values can be significantly reduced when the proposed double exponential distributions in Eq. (3) were used to describe the temperature changes.

Interestingly, the double exponential shape gradually turns counterclockwise, giving rise to a positive skewness in the more recent years (darker lines in Figs. 2a,c). The connection between the mean shift and the apparent clockwise rotation of the exponential tails reveals a coordination between more extreme events and the acceleration of global warming. The change in the PDF properties is summarized by the plots of temperature averages against the standard deviation and the asymmetry index, $\Delta\beta=\beta_1-\beta_2$, a measure of asymmetry of the two tails derived from the fluctuation relations. As shown in Figs. 2b and 2d, the variance is smaller for longer averaging windows and has only a weak dependence on the mean, first decreasing and then increasing for A and gradually increasing for ΔA, whereas the distributions become more asymmetric as the mean increases. Such distributional changes and their profound implications for extreme events can be illustrated in simplified examples in Fig. 4, where shift in standard normal distribution is compared with the asymmetric double exponential distributions with the same means and variances. The negative-to-positive transition in the asymmetry index implies a much higher likelihood of extremely large values at the expense of reduced frequency of very low values. Such deviations from a normal Gaussian pattern have significance for climate modeling validations and should be considered when making predictions and decisions regarding climate-related risks.

It is also interesting to explore the structure of temperature-fluctuation distribution in different regions, which we expect to change due to the different thermodynamic properties of Earth's surface. In general, the role of inhomogeneities in thermodynamic properties is an interesting area that has been

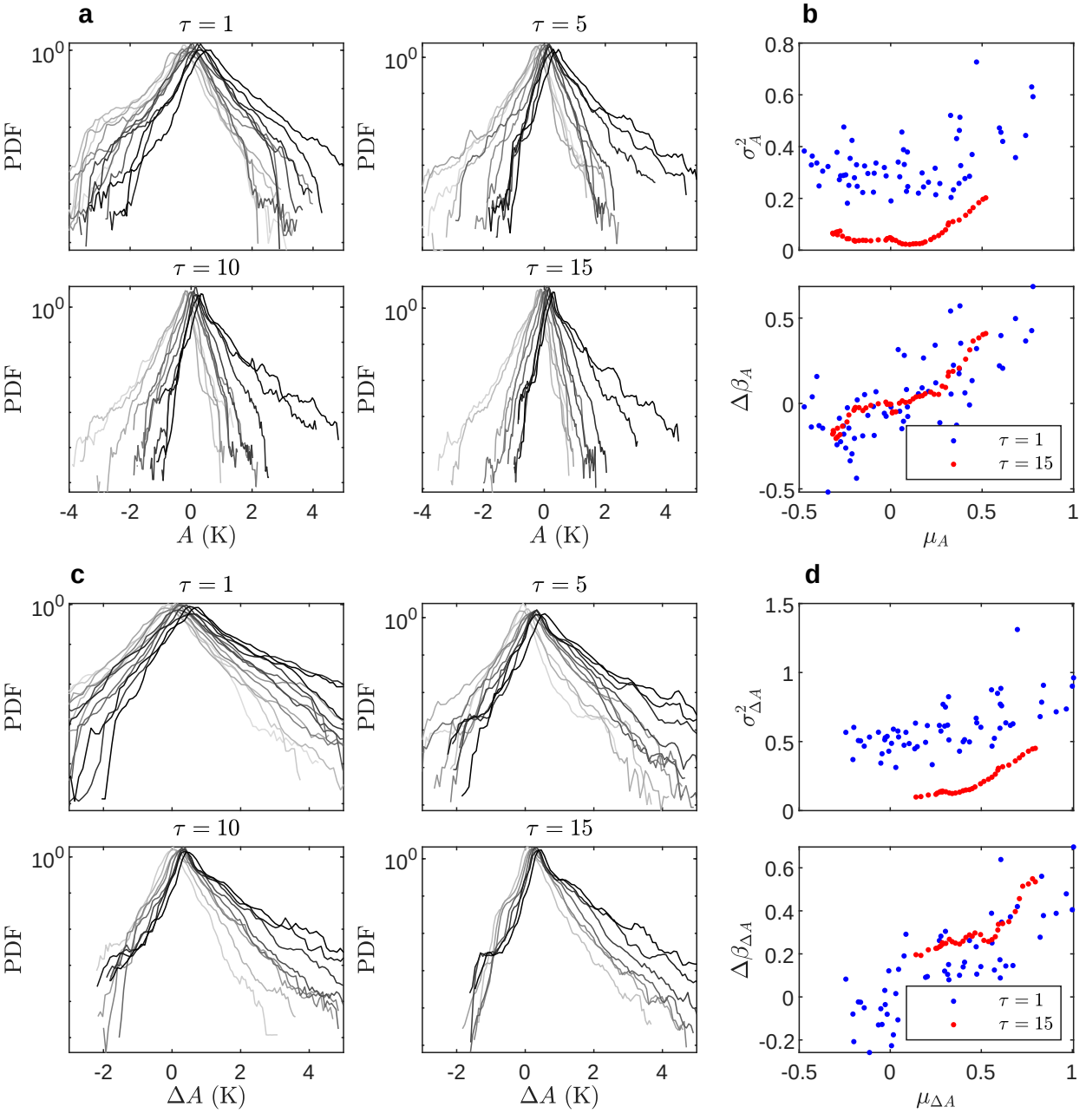

FIG. 2. Global distributions of temperature fluctuations. Probability density functions (PDFs) of (a) anomalies (A) and (c) anomaly differences (ΔA) with different averaging windows (τ) are displayed in chronological order with lighter colors for earlier years (or shorter time differences) and darker colors for the later ones (or longer time differences). The baseline for ΔA is set as the earliest year of the data series. The relationships among mean μ, variances σ^2, and asymmetry $\Delta\beta$ of the (b) anomalies (A) and (d) anomaly differences (ΔA) are presented in blue dots for the short averaging window (τ = 1 year) and in red dots for the long averaging window (τ = 15 years). Results are based on global temperature data during 1959–2021 from ERA5; see similar patterns for other data sources in Fig. S4.

little investigated in statistical mechanics and deserves more attention. In the Earth system analyzed here, the results show that the land temperature distributions tend to move toward the right much faster than those over the ocean (Fig. S6), leading to faster increases in mean temperatures (Fig. 5a). The ocean temperature distributions, with steeper and more irregular exponential tails, appear to rotate counterclockwise faster than those over land (Fig. S7), giving rise to slightly smaller variances and higher skewness (see Figs. 5b,c). This is in general consistent with the observations of slower warming rates over the ocean (e.g., Lenssen et al. 2019) but also highlights the existence of some ocean hotspots with extreme

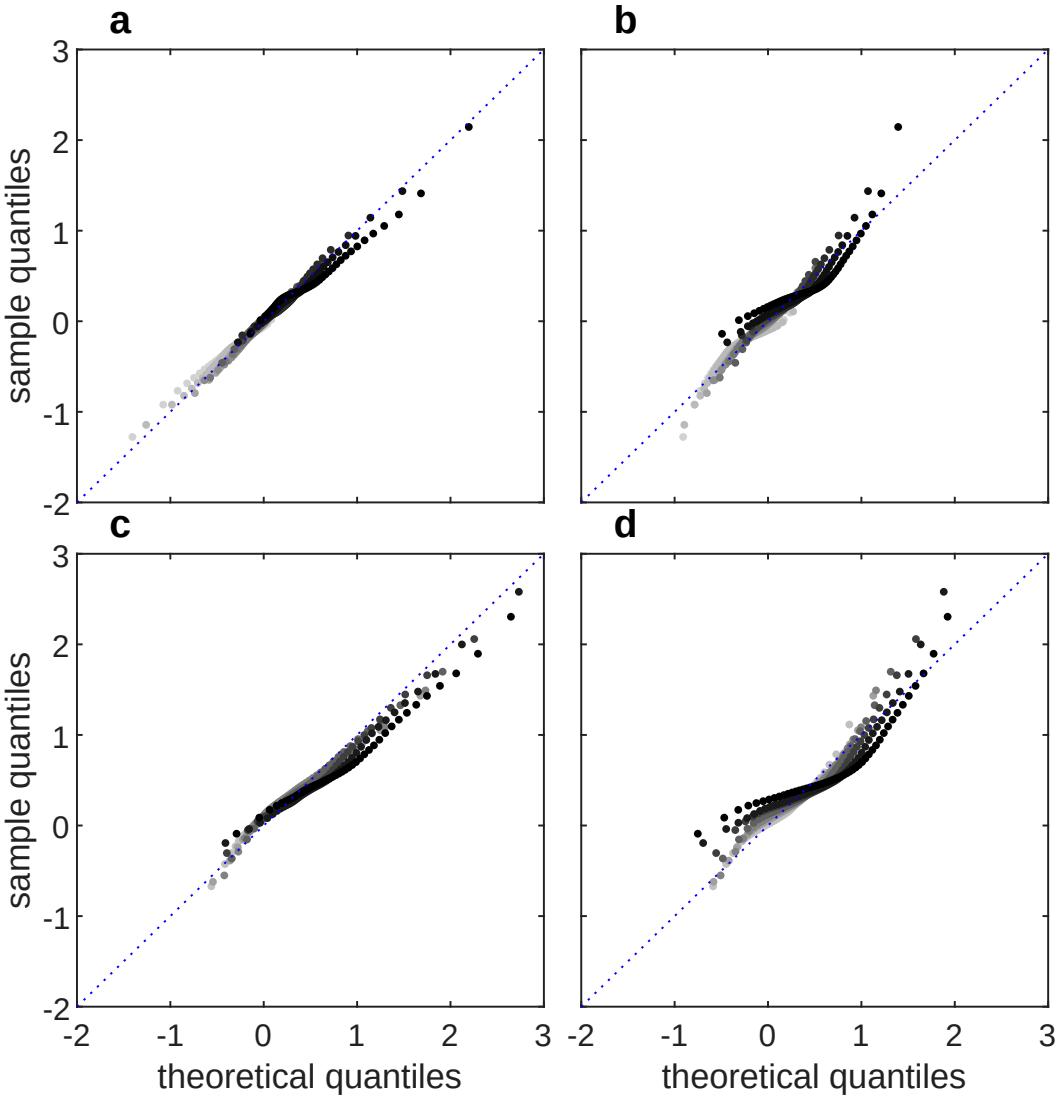

FIG. 3. Quantile–quantile plots for the distributions of (a),(b) temperature anomalies and (c),(d) anomaly differences with averaging windows of 15 years ($\tau = 15$). Quantiles in the y axis (ranging from 1 to 99 with an interval of 2) are from data; quantiles in the x axis are from (a),(c) asymmetric double exponential distributions and (b),(d) Gaussian distributions. The lighter colors refer to A in the earlier years (or shorter time differences) and darker colors refer to the later ones (or longer time differences). Results for $\tau = 1$, 5, and 20 were reported in Fig. S5.

warming rates. With their larger heat capacity and slower responses to the anthropogenic forcing, the oceans in fact are slower to equilibrate, resulting in more asymmetric temperature distributions; on the contrary, warming over the land is closer to a quasi-steady process, leading to simple shifts of temperature distributions with small changes in skewness.

Aside from land and ocean differences, Earth also tends to have higher warming rates near the north pole, a phenomenon known as Arctic amplification (Bekryaev et al. 2010; Stuecker et al. 2018). This is evident in our temperature fluctuation analysis, which shows 1.5 K temperature increases within 30°–90°N over the last four decades but less than 1 K in the rest of the world (see Fig. 5d). While the temperature variances within 30°–90°N decrease before 1980 and then increase after 2000, the variances over the rest of the world keep relatively constant (see Fig. 5e). In contrast, the skewness over each latitudinal band seem to increase approximately at the same rate, presenting different patterns of temperature fluctuations (see Fig. 5f and Figs. S8–S10).

To link this analysis of temperature fluctuations to more conventional approaches, we decompose the local temperature into the forced and random components as

$$T = rt + \eta, \tag{4}$$

where the component (r) is related to the upward warming trend and the random term (η) is associated with the internal climate

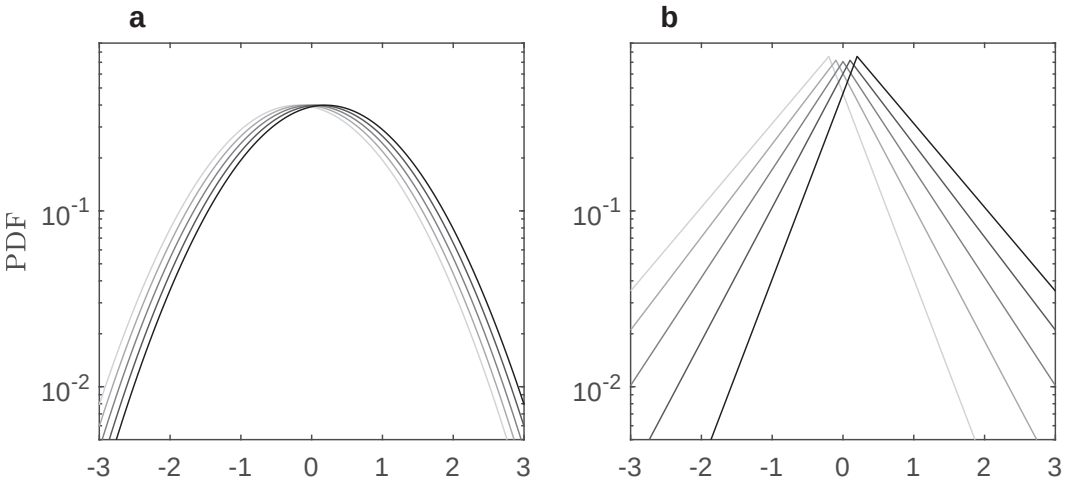

FIG. 4. Schematic representation of the impact of coordination in central tendency shift and tail rotation in temperature distributions compared to a shift in (a) normal (i.e., Gaussian) distributions and (b) the corresponding asymmetric double exponential distributions with the same means and variances but increasing skewness.

variability, which is expected to be smaller at longer time scales. The global distributions of the local warming rates, estimated from the same datasets as before, already show a double exponential shape, which tend to rotate counterclockwise in the more recent years (Fig. S13), suggesting an increase skewness. The anthropogenic origin of this shift is corroborated by the analysis of preindustrial simulations from multiple CMIP6 models. In such unforced experiments, no clear trends in mean, variances, and skewness of the global temperatures were identified after the initial spinup (see Figs. 5g–i and Figs. S11 and S12).

3. Temperature scaling, fluctuation relations, and future projections

As required by fluctuation relations, which concern the asymptotic time averages of fluctuations, we rescaled both sides of the distributions by the corresponding exponents:

$$\bar{x} = \begin{cases} (x - m)/\beta_1, & x > m \\ (x - m)/\beta_2, & x \le m \end{cases}, \tag{5}$$

where the overbar refers to the scaled variable.

After this scaling, the theoretical distribution becomes

$$f(\bar{x}) = \beta_0 \exp(-|\bar{x}|), \tag{6}$$

which has a unit exponent for both tails. The resulting PDFs from data are shown in Figs. 6a and 6c, confirming the almost complete collapse onto a single curve. This allows us to accurately project the global temperature patterns as functions of only three parameters (the two exponents and the mode).

The asymmetry of the distribution with the growth of positive fluctuations at the expense of the negative ones is strongly reminiscent of the symmetry implied by the fluctuation theorem (Evans et al. 1993; Marconi et al. 2008), whereby the ratio of the probabilities taken on opposite signs is related to the dissipation and hence the irreversibility of the nonequilibrium process. As appropriate for large deviation results, we considered the logarithm of the ratio of positive and negative temperature fluctuations away from the mode in a distance of α:

$$\ln\left[\frac{f(\alpha + m)}{f(-\alpha + m)}\right] = \alpha\Delta\beta(\beta_1\beta_2)^{-1}, \tag{7}$$

which turns out to be related to the exponents of the two tails, as one would have predicted from the symmetry of the fluctuation theorem. The results, shown in Figs. 6b and 6d, synthesize the link between the cooling and warming probabilities and the overall warming trend. Its warming-to-cooling ratio, governed by Eq. (7), increases for stronger asymmetric distribution (e.g., longer time differences and more recent years).

The robust scaling of the PDFs and its shift in asymmetry may also be used to extrapolate the data for short lead times to infer global warming trends (see Figs. 7a–c). This was done by fitting the statistics of A with smoothing window $\tau = 15$ to the year 2040. A linear function was first chosen to fit the data but a quadratic function was used to capture the nonlinear behaviors of the variance (see triangles in Figs. 7a–c). This by no means covers all possible extrapolations, but provides a first glimpse into future conditions. Since the mean and variance can be expressed as

$$\mu = m + \beta_1 - \beta_2 \tag{8}$$

and

$$\sigma^2 = \beta_1^2 + \beta_2^2, \tag{9}$$

one can estimate the parameters of the distributions by solving Eqs. (8) and (9) with the definition of asymmetric index as

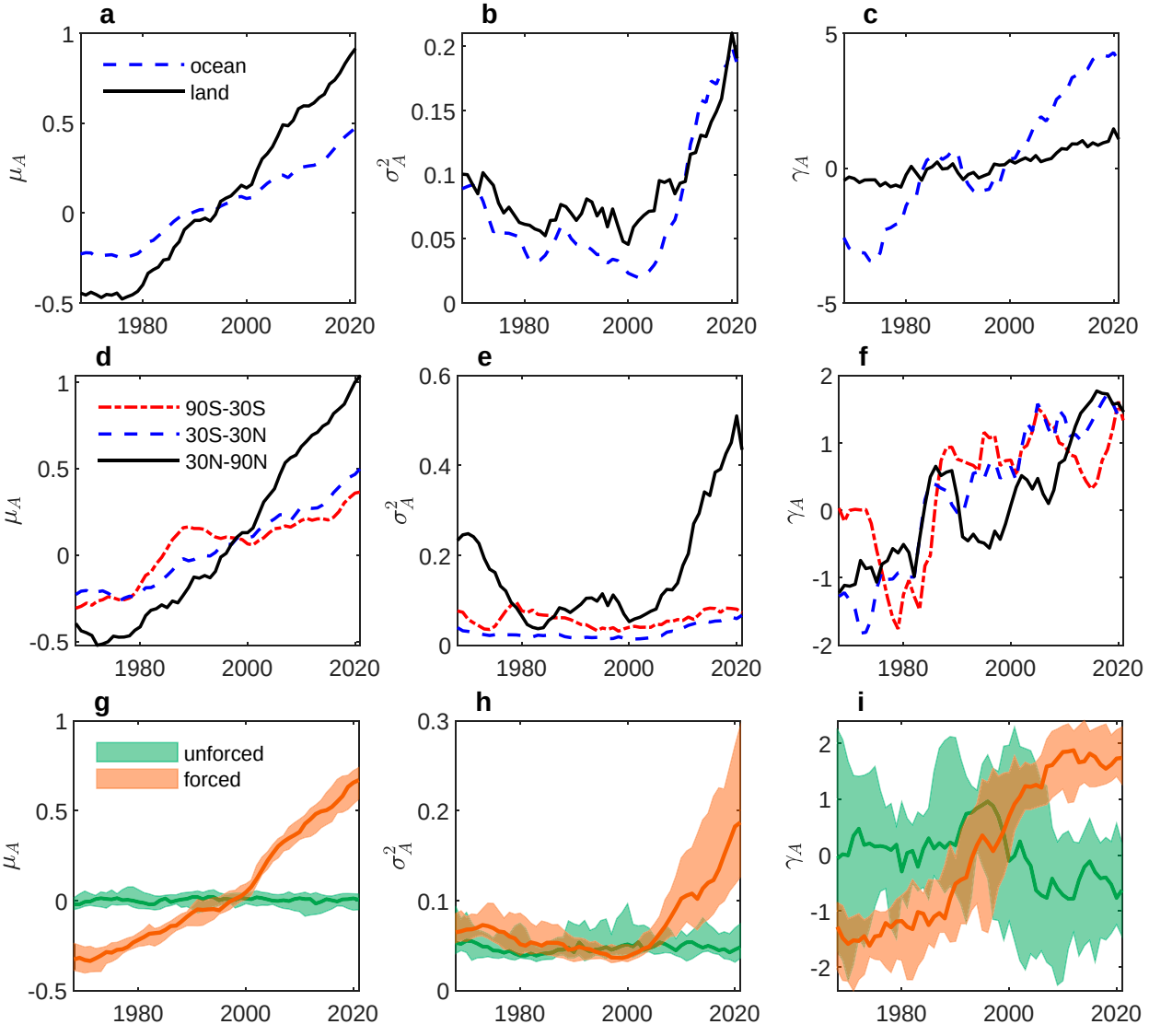

FIG. 5. Time series of (a),(d),(g) mean; (b),(e),(h) variance; and (c),(f),(i) skewness of anomaly with 10-yr averaging window, $A(t, \tau = 10)$, (a)–(c) over the ocean and land and (d)–(f) in different latitudinal bands from reanalysis data, and (g)–(i) over Earth from the forced and unforced climate model simulations. ERA5 data cover 1959–2021; the forced simulations are the "historical" experiments during 1951–2014 and "ssp245" experiments during 2015–21; the unforced simulations refer to 63-yr near-surface temperatures after the initial spinup in the "picontrol" experiment. Model names and experiments are listed in Table S1. Detailed temperature distributions in chronological order are reported in Figs. S6–S12.

$$m = \mu - \Delta\beta,$$
$$\beta_1 = \frac{1}{2}(\sqrt{2\sigma^2 - \Delta\beta^2} + \Delta\beta),$$
$$\beta_2 = \frac{1}{2}(\sqrt{2\sigma^2 - \Delta\beta^2} - \Delta\beta). \quad (12)$$

With the projected mean, variance, and asymmetry index, we can obtain all parameters for the asymmetric double exponential distribution (i.e., m, β_1, β_2) and provide future distributions of temperature anomaly.

Consistent with climate model projections (Masson-Delmotte et al. 2021), the extrapolation shows that a 1.5° mean temperature increase is reached at around 2040, along with an increase in variance and asymmetry. With these statistics, we obtain a distribution of future temperature anomaly, which is extremely skewed, with a shortened left tail and an elongated right tail (see dash lines in Fig. 7d). When compared with climate model outputs (magenta shading and lines) and the observations in recent years, similar patterns are observed, but with a slightly slower increase of skewness in climate models (also see another projection in Fig. S15), showing a certain difficulty in forecasting future extreme events. The simulated temperature distribution around 2040 is generally consistent with our extrapolation results with almost identical right tails, revealing the goodness of the

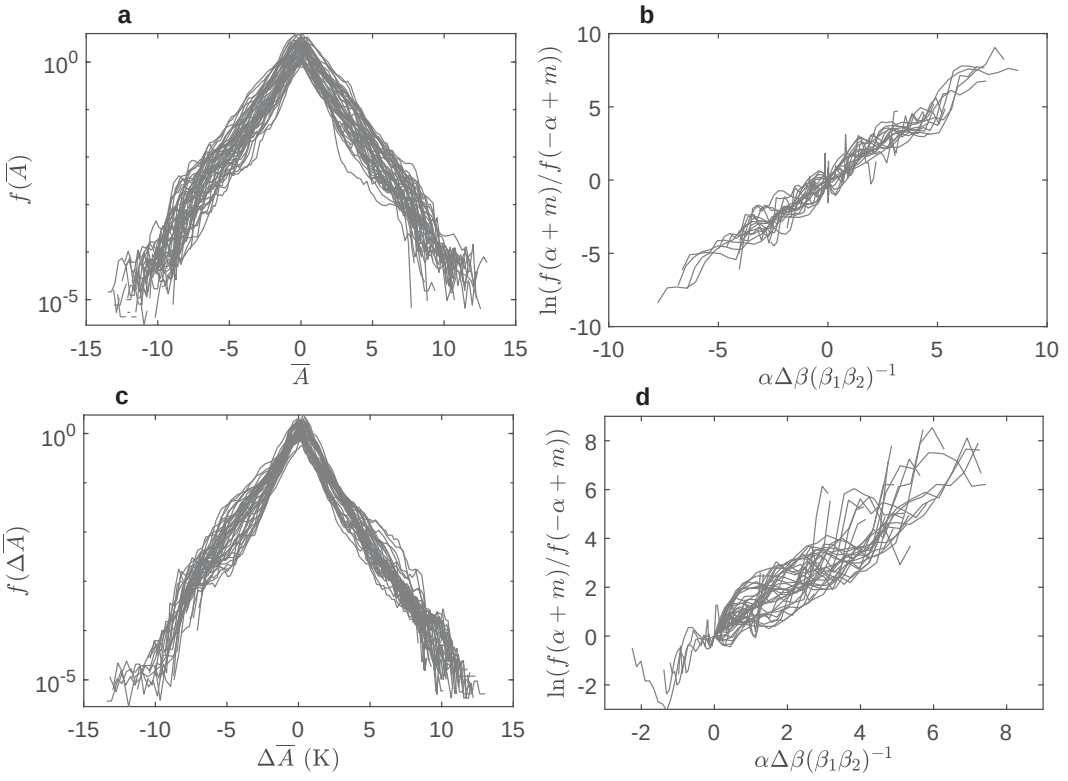

FIG. 6. Rescaling and symmetry of temperature fluctuations. The lines in (a) and (c) are rescaled from the PDFs of A and ΔA in Figs. 2a and 2c, respectively. The tails of these PDFs are linearly stretched to have a unit slope. The symmetry of the temperature fluctuations is evaluated by the ratio of positive and negative temperature fluctuations away from the mode against the differences of the exponents of the tails for (b) A and (d) ΔA. Results are based on ERA5; see similar patterns for other data sources in Fig. S14.

fluctuation approach and corroborating our finding of extreme warming trends in the near future.

The exponential tails are not uncommon for many atmospheric variables, whose time series in certain regions or at point scale may show non-Gaussian distributions (Perron and Sura 2013; Proistosescu et al. 2016; Catalano et al. 2020). Such fat tails may be associated with advection–diffusion process (Pierrehumbert 2000; Neelin et al. 2010) and have important implications for future occurrences of the extreme events (Ruff and Neelin 2012). While these extreme events at regional scales have been described within the framework of Generalized Extreme Value distributions (Cheng et al. 2014) and large deviation theory (Galfi et al. 2019; Galfi and Lucarini 2021; Lucarini et al. 2023), the analysis via the fluctuation theorem discussed here unveils a new perspective on full spectrum of global temperature distributions. Such distributions and its asymmetric temporal shift suggest inevitable increase of probabilities of extreme events in a changing climate. The implications of such spatiotemporal distributions, and the applicability of fluctuation relations for extreme events deserve closer attention, in view of their impact on the large-scale circulation, the hydrological and biogeochemical cycles, as well as ecosystems and society (Easterling et al. 2000; van de Pol et al. 2017).

4. Conclusions

In summary, our analysis based on the fluctuation relation discovered thirty years ago (Evans et al. 1993) uncovered an interesting symmetry of global temperature fluctuations, which is suggestive of a behavior of Earth's climate as a "small" nonequilibrium system. This symmetry, in turn, allowed us to collapse space–time temperature fluctuations into a single scaling law, resulting in a universal shape of the distribution of the temperature anomalies. When extrapolating to the near future, the temperature anomalies present a skewed distribution with elongated tails, highlighting the frequent occurrence of extreme events. An increased impact of climate change appears as a counterclockwise rotation of the temperature distribution tails in a rescaled logarithmic plot (e.g., Fig. 2). The observed asymmetry also provides a logical way to link the shifts in central tendency (mean and variance) of temperature distributions with the tails and higher-order statistics, an important connection to better understand the dynamics and impacts of climate change (Tamarin-Brodsky et al. 2019). The scaling law uncovered here appears very robust and may thus serve as the benchmark for climate model simulations (as seen in Fig. 7d), as well as to infer Earth's response to the changing climates.

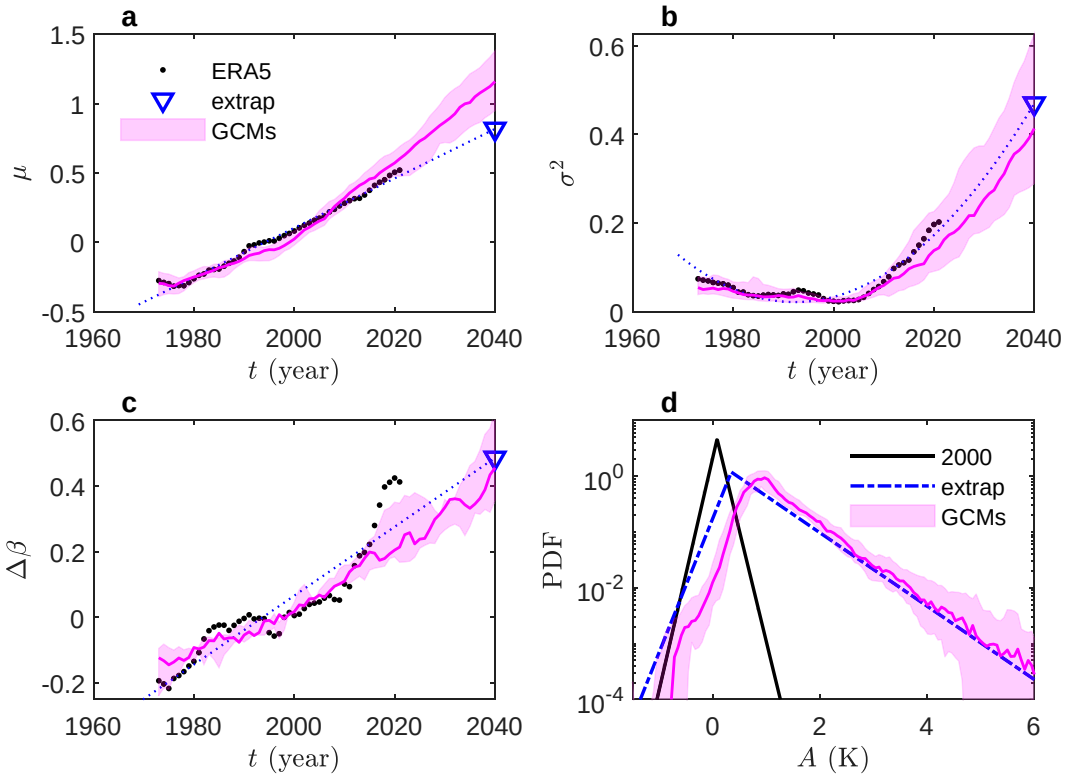

FIG. 7. Future projection of temperature fluctuations. Time series of (a) mean, (b) variance, and (c) asymmetry index of temperature anomalies with an averaging window of 15 years from ERA5 data (thick black dots), compared with those from climate model outputs (magenta shading and lines). Triangles are extrapolation using ERA5 data; results from climate model outputs before and after 2014 were from "historical" and "ssp245" experiments, respectively. A quadratic function was used to capture the nonlinear shape of the variance, whereas linear functions were used for other extrapolations. (d) Distributions of temperature anomalies from climate model outputs (magenta shading and lines) are compared with the asymmetric double exponential distributions, where the mean, variance, and symmetric index were from values in 2000 (black lines) and the extrapolated values in 2040 (dashed lines). The magenta shading marks to the 25th and 75th percentiles of the model outputs and magenta lines show the median values (see Table S1 for model list); results from each climate model are reported in Fig. S16.

While the present analysis has focused on the spatial symmetry of fluctuations at different time scales of aggregation, more detailed analysis should be carried out regarding the asymmetry of temporal fluctuations as well as the local peculiarities of the spatial variability; in particular, the more pronounced tail "rotation" in oceans, in spite of the stronger warming trends observed on land, could be better understood by considering a fine grained spatial picture, which would likely unveil different degrees of tail rotations at different latitudes and specific locations (see, e.g., Bekris et al. 2023, for an analysis of different tail behaviors). Additionally, it should also be noted that changes in the distributional shapes could be seen as precursors of regime shifts, a topic that has been widely pursued in the ecological literature (Guttal and Jayaprakash 2008). It is also natural to wonder whether a particular symmetry in the statistics of the degree of tail rotation exists, whereby the globally positive rotation leading to greater skewness could be deconstructed as the superposition of positive and negative rotations, similar to those predicted by the fluctuation theorem itself.

The similarities of the behaviors of a planetary-scale response with those of small, particle-scale systems not only shed new light on the response of Earth's dynamics to climate change (Ghil and Lucarini 2020), but also opened novel important questions about the universality of fluctuations at different scales. A starting point of this would be a more formal analysis of the fluctuations of Earth's entropy balance. More generally, improved understanding of the origin of the similarities between fluctuation at macroscopic scales (i.e., larger than the continuum scale), such as in turbulence flows (e.g., Porporato et al. 2020), and those at the molecular scale more typical of statistical mechanics (e.g., Lovejoy 2022) could be carried out via controlled laboratory and numerical experiments, where the complications of seasonality and long-term variability can be isolated from the dynamic components related to meteorological and turbulent fluctuations (Seager et al. 2010).

Finally, future work will be also devoted to extending this type of analysis to other important variables, including precipitation and energy-cycle statistics (O'Gorman 2015; Tebaldi et al. 2021), with the goal of harnessing the formalism of

response theory to improve our understanding, simulation, and prediction of the Earth system, especially the all-important question of the changes in distributional tails and the related extreme events (Trenberth 2012).

Acknowledgments. We thank the editor, Robert Jnglin Wills, and two anonymous reviewers, Valerio Lucarini, David Neelin, Gabriel Vecchi, and Paul O'Gorman for their insightful comments and suggestions. J. Y. acknowledges support from the Natural Science Foundation of Jiangsu Province (BK20221343). A. P. acknowledges support from the Carbon Mitigation Initiative at Princeton. L. R. acknowledges financial support by the Ministero dell'Università e della Ricerca (Italy), Grant Dipartimenti di Eccellenza 2018–22 (E11G18000350001). His research was performed under the auspices of Italian National Group of Mathematical Physics (GNFM) of INdAM.

Data availability statement. Data analyzed in this study were a reanalysis of existing data, which are openly available at the following locations: ERA5—https://cds.climate.copernicus.eu/; GISS—https://data.giss.nasa.gov/gistemp/; and CMIP6—https://esgf-node.llnl.gov/search/cmip6/.

REFERENCES

Alexandrov, D. V., I. A. Bashkirtseva, M. Crucifix, and L. B. Ryashko, 2021: Nonlinear climate dynamics: From deterministic behaviour to stochastic excitability and chaos. *Phys. Rep.*, **902**, 1–60, https://doi.org/10.1016/j.physrep.2020.11.002.

Bechinger, C., R. Di Leonardo, H. Löwen, C. Reichhardt, G. Volpe, and G. Volpe, 2016: Active particles in complex and crowded environments. *Rev. Mod. Phys.*, **88**, 045006, https://doi.org/10.1103/RevModPhys.88.045006.

Bekris, Y., P. C. Loikith, and J. D. Neelin, 2023: Short warm distribution tails accelerate the increase of humid-heat extremes under global warming. *Geophys. Res. Lett.*, **50**, e2022GL102164, https://doi.org/10.1029/2022GL102164.

Bekryaev, R. V., I. V. Polyakov, and V. A. Alexeev, 2010: Role of polar amplification in long-term surface air temperature variations and modern Arctic warming. *J. Climate*, **23**, 3888–3906, https://doi.org/10.1175/2010JCLI3297.1.

Bohr, T., and E. B. W. van de Water, 1994: Spatiotemporal chaos. *Nature*, **372**, 48, https://doi.org/10.1038/372048a0.

Bonaldi, M., and Coauthors, 2009: Nonequilibrium steady-state fluctuations in actively cooled resonators. *Phys. Rev. Lett.*, **103**, 010601, https://doi.org/10.1103/PhysRevLett.103.010601.

Brönnimann, S., E. Xoplaki, C. Casty, A. Pauling, and J. Luterbacher, 2007: ENSO influence on Europe during the last centuries. *Climate Dyn.*, **28**, 181–197, https://doi.org/10.1007/s00382-006-0175-z.

Catalano, A. J., P. C. Loikith, and J. D. Neelin, 2020: Evaluating CMIP6 model fidelity at simulating non-Gaussian temperature distribution tails. *Environ. Res. Lett.*, **15**, 074026, https://doi.org/10.1088/1748-9326/ab8cd0.

Cheng, L., A. AghaKouchak, E. Gilleland, and R. W. Katz, 2014: Non-stationary extreme value analysis in a changing climate. *Climatic Change*, **127**, 353–369, https://doi.org/10.1007/s10584-014-1254-5.

Ciliberto, S., and C. Laroche, 1998: An experimental test of the Gallavotti-Cohen fluctuation theorem. *J. Phys. IV Fr.*, **08**, Pr6-215–Pr6-219, https://doi.org/10.1051/jp4:1998629.

Crooks, G. E., 1999: Entropy production fluctuation theorem and the nonequilibrium work relation for free energy differences. *Phys. Rev. E*, **60**, 2721–2726, https://doi.org/10.1103/PhysRevE.60.2721.

Cross, M. C., and P. C. Hohenberg, 1994: Spatiotemporal chaos. *Science*, **263**, 1569–1570, https://doi.org/10.1126/science.263.5153.1569.

Diaz, H. F., M. P. Hoerling, and J. K. Eischeid, 2001: ENSO variability, teleconnections and climate change. *Int. J. Climatol.*, **21**, 1845–1862, https://doi.org/10.1002/joc.631.

Donat, M. G., and L. V. Alexander, 2012: The shifting probability distribution of global daytime and night-time temperatures. *Geophys. Res. Lett.*, **39**, L14707, https://doi.org/10.1029/2012GL052459.

Easterling, D. R., J. L. Evans, P. Y. Groisman, T. R. Karl, K. E. Kunkel, and P. Ambenje, 2000: Observed variability and trends in extreme climate events: A brief review. *Bull. Amer. Meteor. Soc.*, **81**, 417–426, https://doi.org/10.1175/1520-0477(2000)081<0417:OVATIE>2.3.CO;2.

Evans, D. J., and D. J. Searles, 2002: The fluctuation theorem. *Adv. Phys.*, **51**, 1529–1585, https://doi.org/10.1080/00018730210155133.

——, and G. Morriss, 2008: *Statistical Mechanics of Nonequilibrium Liquids*. 2nd ed. Cambridge University Press, 314 pp.

——, E. G. D. Cohen, and G. P. Morriss, 1993: Probability of second law violations in shearing steady states. *Phys. Rev. Lett.*, **71**, 2401–2404, https://doi.org/10.1103/PhysRevLett.71.2401.

Franzke, C. L. E., and Coauthors, 2020: The structure of climate variability across scales. *Rev. Geophys.*, **58**, e2019RG000657, https://doi.org/10.1029/2019RG000657.

Galfi, V. M., and V. Lucarini, 2021: Fingerprinting heatwaves and cold spells and assessing their response to climate change using large deviation theory. *Phys. Rev. Lett.*, **127**, 058701, https://doi.org/10.1103/PhysRevLett.127.058701.

——, ——, and J. Wouters, 2019: A large deviation theory-based analysis of heat waves and cold spells in a simplified model of the general circulation of the atmosphere. *J. Stat. Mech.: Theory Exp.*, **2019**, 033404, https://doi.org/10.1088/1742-5468/ab02e8.

Gallavotti, G., 2014: *Nonequilibrium and Irreversibility*. Springer, 244 pp.

——, and E. G. D. Cohen, 1995: Dynamical ensembles in nonequilibrium statistical mechanics. *Phys. Rev. Lett.*, **74**, 2694–2697, https://doi.org/10.1103/PhysRevLett.74.2694.

——, L. Rondoni, and E. Segre, 2004: Lyapunov spectra and nonequilibrium ensembles equivalence in 2D fluid mechanics. *Physica D*, **187**, 338–357, https://doi.org/10.1016/j.physd.2003.09.029.

Ghil, M., and V. Lucarini, 2020: The physics of climate variability and climate change. *Rev. Mod. Phys.*, **92**, 035002, https://doi.org/10.1103/RevModPhys.92.035002.

Guttal, V., and C. Jayaprakash, 2008: Changing skewness: An early warning signal of regime shifts in ecosystems. *Ecol. Lett.*, **11**, 450–460, https://doi.org/10.1111/j.1461-0248.2008.01160.x.

Hansen, J., M. Sato, and R. Ruedy, 2012: Perception of climate change. *Proc. Natl. Acad. Sci. USA*, **109**, E2415–E2423, https://doi.org/10.1073/pnas.1205276109.

Huybers, P., K. A. McKinnon, A. Rhines, and M. Tingley, 2014: U.S. daily temperatures: The meaning of extremes in the context of nonnormality. *J. Climate*, **27**, 7368–7384, https://doi.org/10.1175/JCLI-D-14-00216.1.

Jarzynski, C., 2004: Nonequilibrium work theorem for a system strongly coupled to a thermal environment. *J. Stat. Mech.: Theory Exp.*, **2004**, P09005, https://doi.org/10.1088/1742-5468/2004/09/P09005.

Kleidon, A., 2016: *Thermodynamic Foundations of the Earth System*. Cambridge University Press, 379 pp.

Klein, R., 2010: Scale-dependent models for atmospheric flows. *Annu. Rev. Fluid Mech.*, **42**, 249–274, https://doi.org/10.1146/annurev-fluid-121108-145537.

Kozubowski, T. J., and K. Podgórski, 2000: A multivariate and asymmetric generalization of Laplace distribution. *Comput. Stat.*, **15**, 531–540, https://doi.org/10.1007/PL00022717.

Lenssen, N. J. L., G. A. Schmidt, J. E. Hansen, M. J. Menne, A. Persin, R. Ruedy, and D. Zyss, 2019: Improvements in the GISTEMP uncertainty model. *J. Geophys. Res. Atmos.*, **124**, 6307–6326, https://doi.org/10.1029/2018JD029522.

Lewis, S. C., and A. D. King, 2017: Evolution of mean, variance and extremes in 21st century temperatures. *Wea. Climate Extremes*, **15**, 1–10, https://doi.org/10.1016/j.wace.2016.11.002.

Lovejoy, S., 2022: The 2021 "complex systems" Nobel prize: The climate, with and without geocomplexity. *AGU Adv.*, **3**, e2021AV000640, https://doi.org/10.1029/2021AV000640.

Lu, J., G. A. Vecchi, and T. Reichler, 2007: Expansion of the Hadley cell under global warming. *Geophys. Res. Lett.*, **34**, L06805, https://doi.org/10.1029/2006GL028443.

Lucarini, V., V. M. Galfi, J. Riboldi, and G. Messori, 2023: Typicality of the 2021 western North America summer heatwave. *Environ. Res. Lett.*, **18**, 015004, https://doi.org/10.1088/1748-9326/acab77.

Marconi, U. M. B., A. Puglisi, L. Rondoni, and A. Vulpiani, 2008: Fluctuation–dissipation: Response theory in statistical physics. *Phys. Rep.*, **461**, 111–195, https://doi.org/10.1016/j.physrep.2008.02.002.

Marotzke, J., and P. M. Forster, 2015: Forcing, feedback and internal variability in global temperature trends. *Nature*, **517**, 565–570, https://doi.org/10.1038/nature14117.

Masson-Delmotte, V., and Coauthors, 2021: *Climate Change 2021: The Physical Science Basis*. Cambridge University Press, 2409 pp.

Neelin, J. D., B. R. Lintner, B. Tian, Q. Li, L. Zhang, P. K. Patra, M. T. Chahine, and S. N. Stechmann, 2010: Long tails in deep columns of natural and anthropogenic tropospheric tracers: Long tails in tropospheric tracers. *Geophys. Res. Lett.*, **37**, L05804, https://doi.org/10.1029/2009GL041726.

O'Gorman, P. A., 2015: Precipitation extremes under climate change. *Curr. Climate Change Rep.*, **1**, 49–59, https://doi.org/10.1007/s40641-015-0009-3.

Perron, M., and P. Sura, 2013: Climatology of non-Gaussian atmospheric statistics. *J. Climate*, **26**, 1063–1083, https://doi.org/10.1175/JCLI-D-11-00504.1.

Pierrehumbert, R. T., 2000: Lattice models of advection-diffusion. *Chaos*, **10**, 61–74, https://doi.org/10.1063/1.166476.

Porporato, A., M. Hooshyar, A. D. Bragg, and G. Katul, 2020: Fluctuation theorem and extended thermodynamics of turbulence. *Proc. Roy. Soc.*, **476A**, 20200468, https://doi.org/10.1098/rspa.2020.0468.

Proistosescu, C., A. Rhines, and P. Huybers, 2016: Identification and interpretation of nonnormality in atmospheric time series. *Geophys. Res. Lett.*, **43**, 5425–5434, https://doi.org/10.1002/2016GL068880.

Ruff, T. W., and J. D. Neelin, 2012: Long tails in regional surface temperature probability distributions with implications for extremes under global warming. *Geophys. Res. Lett.*, **39**, L04704, https://doi.org/10.1029/2011GL050610.

Seager, R., N. Naik, and G. A. Vecchi, 2010: Thermodynamic and dynamic mechanisms for large-scale changes in the hydrological cycle in response to global warming. *J. Climate*, **23**, 4651–4668, https://doi.org/10.1175/2010JCLI3655.1.

Seifert, U., 2012: Stochastic thermodynamics, fluctuation theorems and molecular machines. *Rep. Prog. Phys.*, **75**, 126001, https://doi.org/10.1088/0034-4885/75/12/126001.

Stefanova, L., P. Sura, and M. Griffin, 2013: Quantifying the non-Gaussianity of wintertime daily maximum and minimum temperatures in the Southeast. *J. Climate*, **26**, 838–850, https://doi.org/10.1175/JCLI-D-12-00161.1.

Stuecker, M. F., and Coauthors, 2018: Polar amplification dominated by local forcing and feedbacks. *Nat. Climate Change*, **8**, 1076–1081, https://doi.org/10.1038/s41558-018-0339-y.

Tamarin-Brodsky, T., K. Hodges, B. J. Hoskins, and T. G. Shepherd, 2019: A dynamical perspective on atmospheric temperature variability and its response to climate change. *J. Climate*, **32**, 1707–1724, https://doi.org/10.1175/JCLI-D-18-0462.1.

Tebaldi, C., and Coauthors, 2021: Extreme sea levels at different global warming levels. *Nat. Climate Change*, **11**, 746–751, https://doi.org/10.1038/s41558-021-01127-1.

Trenberth, K. E., 2012: Framing the way to relate climate extremes to climate change. *Climatic Change*, **115**, 283–290, https://doi.org/10.1007/s10584-012-0441-5.

——, J. T. Fasullo, and T. G. Shepherd, 2015: Attribution of climate extreme events. *Nat. Climate Change*, **5**, 725–730, https://doi.org/10.1038/nclimate2657.

van de Pol, M., S. Jenouvrier, J. H. C. Cornelissen, and M. E. Visser, 2017: Behavioural, ecological and evolutionary responses to extreme climatic events: Challenges and directions. *Philos. Trans. Roy. Soc.*, **B372**, 20160134, https://doi.org/10.1098/rstb.2016.0134.

Yu, K., and J. Zhang, 2005: A three-parameter asymmetric Laplace distribution and its extension. *Commun. Stat.*, **34**, 1867–1879, https://doi.org/10.1080/03610920500199018.